ELSEVIER

Journal of Nuclear Materials 258–263 (1998) 640–644

journal of nuclear materials

Tritium saturation in plasma-facing materials surfaces [1]

Glen R. Longhurst [a,*], Robert A. Anderl [a], Rion A. Causey [b], Gianfranco Federici [c], Anthony A. Haasz [d], Robert J. Pawelko [a]

[a] *Idaho National Engineering and Environmental Laboratory, Idaho Falls, Idaho, USA*
[b] *Sandia National Laboratories, Livermore, CA, USA*
[c] *ITER Garching Joint Work Site, Garching, Germany*
[d] *Institute for Aerospace Studies, University of Toronto, Toronto, Ont., Canada*

Abstract

Plasma-facing components in the International Thermonuclear Experimental Reactor (ITER) will experience high heat loads and intense plasma fluxes of order 10^{20}–10^{23} particles/m^{2}s. Experiments on Be and W, two of the materials considered for use in ITER, have revealed that a tritium saturation phenomenon can take place under these conditions in which damage to the surface results that enhances the return of implanted tritium to the plasma and inhibits uptake of tritium. This phenomenon is important because it implies that tritium inventories due to implantation in these plasma-facing materials will probably be lower than was previously estimated using classical recombination-limited release at the plasma surface. Similarly, permeation through these components to the coolant streams should be reduced. In this paper we discuss evidences for the existence of this phenomenon, describe techniques for modeling it, and present results of the application of such modeling to prior experiments.

1. Introduction

Plasma-facing components of the International Thermonuclear Experimental Reactor (ITER) must be specially designed to withstand high heat loads and at the same time avoid contamination of the plasma by sputter-erosion of the material surface [1]. Plans for the ITER Basic Performance Phase call for the first wall in the main plasma chamber to be constructed of Be-clad Cu with stainless-steel coolant channel liners and backing shield structure. In areas such as the baffles where fluxes and heat loads are high, similar construction is planned but with possible W cladding to provide longer lifetime under erosion conditions than would be given by Be. Within the divertor, carbon fiber composite material will protect the surfaces near the strike points, subjected to the highest heat loads, with tungsten used elsewhere.

During operation, carbon may coat interior surfaces in which case tritium retention will be as if it were a carbon-lined machine, and a significant portion of the tritium entering the machine will be retained. Previous estimates of tritium inventories in the ITER plasma-facing component (PFC) surfaces and present design estimates assume that will not be the case for the first wall. The degree to which the metal surfaces will be free of contaminants such as C and O will depend on plasma purity, surface temperatures, and particle flux parameters, but present estimates are that first wall and baffle surfaces will be clean.

Previously analysts had assumed that re-emission of tritium implanted into Be- and W-clad PFCs would follow classical concepts of diffusion to the surface followed by recombination. Experiments with Be at low ion fluxes had shown that behavior, but varying recombination coefficients had been estimated [2,3]. Similarly, W experiments had resulted in the conclusion of recombination-limited re-emission, and again, differing transport parameters were found [4,5]. Tritium inventory in ITER PFCs using these concepts had been estimated to be more than 1 kg [6,7]. Recent experimental

* Corresponding author.

[1] This work was supported by the US Department of Energy, Office of Energy Research, Office of Fusion Energy Sciences under DOE Contract No. DE-AC07-94ID13223.

0022-3115/98/$19.00
PII: S0022-3115(98)00112-3

evidence for Be is convincing that it will be much less than that because of saturation effects at the high particle fluxes expected in ITER [8]. Similar results are beginning to appear for W, [9–12] but it is too early in that development to warrant firm conclusions. Therefore, we focus here on saturation in Be. We review that evidence, suggest ways of modeling that behavior, and show that such a model gives good agreement with a wide range of experiments.

2. Experimental observations

It is known that Be saturates with hydrogen under ion bombardment [8,13,14] Chernikov et al. [15] showed graphic evidence of the formation and growth of bubbles during implantation of Russian TIP-30 Be with 3- and 10-keV deuterons at fluences ranging from 3×10^{20} to 8×10^{21} D/m^2. Sample temperatures were 300, 500, and 700 K. Guseva et al. [16] exposed Russian TShP Be (98.7 wt% Be, 0.9 wt% O, 0.2 wt% Fe) to 5-keV H ions with flux density 6.2×10^{21} H/m^{2}s in the SAPPHIRE facility. They reported that elastic recoil detection and secondary ion mass spectroscopy measurements of the hydrogen profile showed an unexpected reduction in the inventory of implanted hydrogen and a shift of the spatial distribution of that hydrogen toward the surface with increasing ion fluence. After a fluence of 2.3×10^{23} H/m^2, surface pits were observed to develop mostly along grain boundaries. After 1.2×10^{24} H/m^2, erosion cones were beginning to form, and by 1.5×10^{25} H/m^2, cones had grown to an advanced stage with the surface under the cones taking on a rather amorphous appearance.

Additional insight was gained from recent experiments on the Tritium Plasma Experiment at Los Alamos National Laboratory [17]. Five-cm diameter disks of hot-pressed and sintered S-65 Be, 2 mm thick were exposed to fluxes of deuterium ions with a 3% tritium tracer. Plasma currents of 0.8–9.2 A gave fluxes from 2.5×10^{21} to 2.8×10^{22} (D+T)/m^{2}s at ion energies of about 100 eV. Exposures lasted one hour with samples maintained at constant temperatures from 100°C to 700°C. Following the implantation, the samples were cooled, transported through air to a separate outgasing furnace and subjected to thermal desorption tests in which the samples were thermally ramped in a flowing mixture of helium and 1% hydrogen. Temperatures were increased from room temperature to 800°C at a constant ramp rate of 20°C/min. Tritium retention was measured by counting the tritium activity in glycol bubblers through which the gas stream passed, and overall hydrogen content was estimated by extrapolation using the known D/T ratio in the implanting gas. Post- experiment observation of samples under a scanning electron microscope revealed the surface was ''hairy'' from formation of many slender and closely spaced sputter-erosion cones.

Experiments on samples exposed to similar ion fluxes (no tritium) at 200°C and 500°C in the PISCES-B facility at the University of California San Diego used nuclear reaction analysis to profile the concentration of implanted deuterium and measure areal densities [18].

Experiments [19] conducted at the Idaho National Engineering and Environmental Laboratory (INEEL) in the early 1990s were characterized by implantation fluxes of $(5 - 6) \times 10^{19}$ D/m^{2}s at 1 keV/D and sample temperatures of the order of 475°C. The samples were 25–71 μm thick. The plasma-side surfaces of the foils were found to have severe damage and pitting to a depth of 1 μm following the experiments. These may have been bubbles uncovered by erosion. Other work in concert with Sandia National Laboratories [20] and subsequent investigations at the INEEL [21] investigated tritium retention and release in neutron irradiated Be.

Implantations of 1-keV D^+ ions into polycrystalline Be at 27°C over a fluence range of 10^{21} to 5×10^{24} D/m^2 show that for fluences greater than 10^{22} D/m^2 the D retention tends to saturation [9]. Observations from these experiments regarding hydrogen ion implantation in Be include the following points.

1. Hydrogen isotopes exist in both molecular and atomic forms in ion-implanted Be and in neutron-irradiated Be [15,20,21]. Much if not most hydrogen is molecular, appearing to reside in bubbles. Single atoms are probably attached to free Be surfaces or to BeO or other impurities [12].
2. Hydrogen concentration from ion implantation saturates in Be. Causey [17] observed that the saturation concentration depends on temperature but hardly at all on ion flux. Wampler [13] observed an atom concentration of 0.31 D/Be for room-temperature implantation with 500 and 1,500 eV deuterons. These findings are consistent with the room-temperature 'saturation' values of about 0.39 D/Be ($(2 - 3) \times 10^{21}$ D/m^2) reported by Haasz and Davis [9]. Chernikov et al. [15] found that saturation of 10-keV D in Be at 700 K was 0.005–0.01 atom fraction. Saturation appeared to grow from the implantation zone to the surface, possibly a consequence of erosion of the surface. Mayer et al. [22] found that in ambient temperature BeO, hydrogen appears to saturate at 0.38 H/Be. Recombination/re-emission occurs very quickly once saturation reaches the surface [15].
3. Gas pressure in the bubbles appears to be very close to equilibrium values [15].
4. There is a damage region much deeper than the implantation zone where traps are more numerous than they are in the bulk of the Be [15,19]. The extent of this region appears to correlate with implanting ion energy.

5. Films of impurities such as carbon and oxygen can form on the plasma-facing surface at all practical operating pressures [23]. At elevated temperatures (above 200°C) beryllium may diffuse through the surface films to form compounds (e.g., Be_2C or BeO) or mixed material layers. In many experiments involving hydrogen transport in Be, the rate-limiting processes are associated with surface films [24]. Such films can alter sputter yields [25].
6. Diffusivities for mobile atoms in Brush Wellman S-65 Be appear to fit those given by Abramov's [26] expression for high grade Be. Diffusivity of deuterium in single crystal Be is much lower than the effective diffusivity in polycrystalline Be [27]. Differences between the high diffusivities measured by Abramov and other values (e.g., Jones and Gibson [28]) can be reconciled as due to the effect of traps.
7. Surface erosion, a separate process from saturation, has a non-negligible effect on tritium inventory near the surface under high ion fluxes [19,29,30].

3. Modeling transport processes

The saturation process is important because it limits the inventory and permeation rate in surfaces exposed to high ion fluxes where it is operative. As the surface of the material becomes saturated with implanted hydrogen isotope atoms, the hydrogen precipitates into bubbles, and the bubbles grow and interconnect to form channels for the rapid return of implanted ions to the plasma. That effectively bypasses the rate-limiting process of recombination, or, equivalently, it makes the recombination coefficient become very large. That appears to place an upper bound on the mobile atom concentration near the surface. Hence, the diffusion and trapping that otherwise would occur in the bulk material are retarded. That has a very favorable effect on tritium inventories and permeation rates to coolant streams.

TMAP4 [31], Diffuse [32], PIDAT [33] and other codes use the same transport equations for modeling movement of hydrogen isotopes through materials. However, these codes were not written to deal with saturation. Determining how to model saturation using these codes and thus to extrapolate experimental results to operating fusion machines is a topic for this work. A single diffusing species is assumed here, but the extension to multiple species is straightforward.

Under a solution-law-dependent or a fixed-concentration boundary condition, surface fluxes are calculated from

$$J_i = -D\left(\nabla n + \frac{nQ^*}{kT^2}\nabla T\right) - un, \tag{1}$$

where D is the diffusivity, n is the concentration of diffusing atoms, k is Boltzmann's constant, T is temperature, and the second term in parentheses accounts for the Ludwig–Soret effect (mass transport due to a temperature gradient), characterized by the heat of transport Q^*. The erosion face velocity is signified by u. The last term may be needed to adjust for the erosion loss that will usually accompany saturation at the high fluxes where saturation applies.

When recombination is rate-limiting, the total flux of mobile hydrogen ions to the surface is

$$J_i = -\left(2K_r n_0^2 + un_0\right). \tag{2}$$

Here n_0 is the mobile atom concentration at the surface, and the negative sign indicates that the recombination current is in the negative x direction for positive erosion-face velocity u. The second term accounts for hydrogen removed from the plasma-exposed face as erosion takes place. In many instances it is negligible. Under ITER-like conditions it becomes noticeable.

A change can be made in K_r to accommodate saturation and erosion. This may be accomplished by allowing the recombination coefficient to grow exponentially when the surface concentration reaches the saturation level. The resulting equation for K_r for Be is

$$K_r = \left[3.4\text{E}-29\ \exp\left(\frac{-0.28\ \text{eV}}{kT}\right)\right] \times \left[1+\exp\left(\frac{10n_0}{n_{sat}} - 10\right)\right] + \frac{u}{1+n_0}. \tag{3}$$

Here the first term in brackets is the Hsu–Andrew–Causey [34] value for the recombination coefficient obtained at low fluxes. The term in the second set of brackets accomplishes exponential growth at saturation. The abruptness of growth (factor of 10 here) is somewhat arbitrary and remains to be determined experimentally. The last term accommodates loss of hydrogen from the surface by surface erosion. The term n_0 is the surface mobile atom concentration while n_{sat} is the saturation value of the hydrogen atom concentration in the material.

In the determination of n_{sat}, it is often assumed that the pressure (fugacity if real gas laws are assumed) of hydrogen in the bubbles will be in equilibrium with the surface tension of the bubble interface. Some argue that a better approach is to identify the hydrogen pressure with that required to punch dislocation loops from the bubble [35]. Because of the severe non-equilibrium associated with implantation from ITER-like plasmas and the great distortions from regular crystal structures evident in photomicrographs, our preferred way of looking at that condition is to say that when the pressure in the bubble exceeds the yield stress of the material, the bubble will grow reducing the pressure. This is particularly to be expected for the large bubbles observed, where surface tension effects will be small. Hence, the

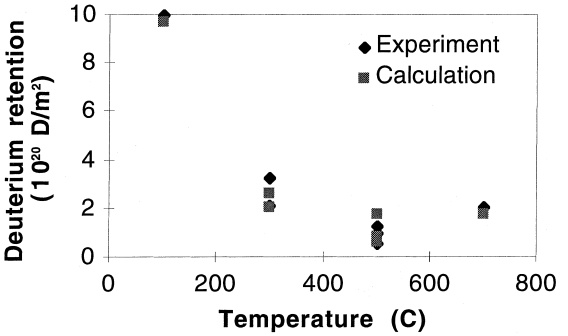

Fig. 1. TMAP4 modeling of the TPE experiments [17] allowing for saturation and erosion as described in the text.

yield stress of the material is taken to correspond to the limiting pressure in the bubbles. Using Sieverts' law, one may then relate the pressure in the bubbles to the concentration of mobile hydrogen in the vicinity of the implantation zone [36]. It is the product of the square root of material yield stress [37] and solubility [38]. The Be result is

$$n_{\mathrm{sat}} = \frac{4.079 \times 10^{26}}{\left[1 + 0.0012T + \left(\frac{T}{950}\right)^{16}\right]^{1/2}} \exp\left(\frac{0.17\ \mathrm{eV}}{kT}\right) \left(\frac{\mathrm{atom}}{\mathrm{m}^3}\right). \quad (4)$$

That value becomes the driving potential for diffusion of hydrogen into the bulk of the beryllium.

4. Simulating experiments

Using the TMAP4 code with the modifications just described, the experiments of Causey on the TPE [17] described in Section 2 were simulated. Agreement between calculated and measured retention was quite good as shown in Fig. 1. The multiple points at the various temperatures represent multiple experiments with widely differing particle fluxes at those temperatures. For comparison, another experiment modeled was that of Hsu et al. [39] which did not exhibit saturation effects, but the saturation model developed was used in the simulation. Fig. 2 shows the best fit line to their data and the agreement achieved with calculations. In the experiments of Anderl et al. [19], saturation effects were clearly evident. Fig. 3 shows the agreement obtained by applying the same saturation model to those experiments. Application of this same model to the ITER first wall and upper baffle shows that breakthrough will not take place during the Basic Performance Phase. Inventories in the Be first wall will be on the order of 100 g rather than the kilogram quantities estimated previous-

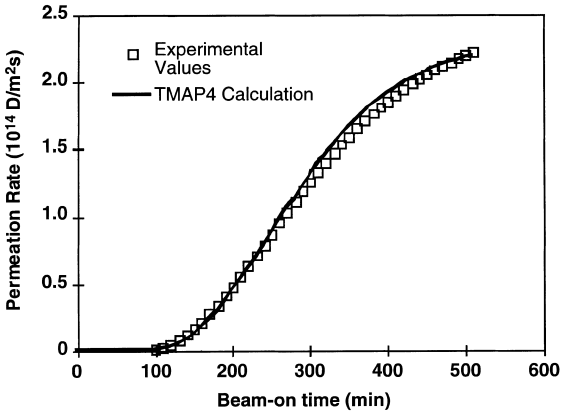

Fig. 3. TMAP4 simulation of INEEL permeation experiment on Be [19].

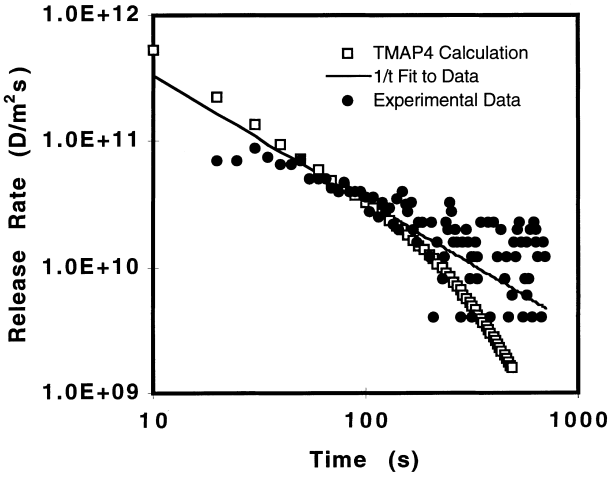

Fig. 2. TMAP4 simulation of the experiment of Hsu et al. [2] using the same saturation model that fit the Causey et al. [17] experiments.

ly, and most of that will come by neutron transmutations in the Be itself.

5. Conclusions

Experimental results surveyed combined with simulations of those experiments using the TIMAP4 code have shown that at high ion fluxes saturation of hydrogen occurs in Be plasma-facing surfaces. The value of including this process in making estimates of tritium inventories in PFCs is that saturation has the effect of limiting the rate at which tritium from the plasma can be absorbed by the structures in which it takes place. Saturation can be effectively modeled by allowing the recombination coefficient to become exponentially large as the mobile atom concentration near the plasma-facing surface approaches a critical value. For Be, calculation results suggest the critical concentration is related to the yield strength using Sieverts' law solubility.

References

[1] Technical basis for the ITER detail design report, Cost review and safety analysis (DDR), International thermonuclear experimental reactor project, Draft, 12, 1996, Final to be published by the International Atomic Energy Agency.
[2] W.L. Hsu et al., J. Nucl. Mater. 176/177 (1990) 218.
[3] G. Saibene et al., J. Nucl. Mater. 176/177 (1990) 618.
[4] R.A. Anderl et al., Fusion Technology 21 (1992) 745.
[5] P. Franzen et al., J. Nucl. Mater. 341–243 (1997) 1082.
[6] G. Federici et al., Proceedings 16th IEEE/NPSS Symposium on Fusion Engineering, Champaign-Urbana, Illinois, 0-7803-2969-4/95, 1995, p. 418.
[7] G.R. Longhurst et al., Fusion. Technol. 28 (1995) 1217.
[8] G. Federici et al., Proc. ISFNT-4, Tokyo, Fusion. Eng. Design, 1997, to appear.
[9] A.A. Haasz, J.W. Davis, J. Nucl. Mater. 241–243 (1997) 1076.
[10] H. Eleveld, Hydrogen and helium in selected fusion reactor materials, Doctoral Thesis, Technische Universiteit Delft, The Netherlands, 1996.
[11] R.A. Anderl et al., Fusion Technol. 21 (1992) 745.
[12] V.Kh. Alimov et al., J. Nucl. Mater. 241–243 (1997) 1047.
[13] W.R. Wampler, J. Nucl. Mater. 122/123 (1984) 1598.
[14] W.R. Wampler, J. Nucl. Mater. 196–198 (1992) 981.
[15] V.N. Chernikov, V.Kh. Alimov, A.P. Zakharov, J. Nucl. Mater. 228 (1996) 47.
[16] M.I. Guseva et al., CONF-9509218, Idaho National Engineering and Environmental Laboratory, 1995.
[17] R.A. Causey et al., J. Nucl. Mater. 241–243 (1997)1041.
[18] W.R. Wampler, unpublished data.
[19] R.A. Anderl et al., J. Nucl. Mater. 196–198 (1992) 986.
[20] J.M. Beeston et al., EGG-FSP-9125, Idaho National Engineering and Environmental Laboratory, 1990.
[21] R.A. Anderl et al., J. Fusion Energy 16 (1997) 101.
[22] M. Mayer et al., J. Nucl. Mater. 230 (1996) 67.
[23] Unpublished INEEL experimental data.
[24] R.G. Macaulay-Newcombe et al., J. Nucl. Mater. 191–194 (1992) 263.
[25] J. Won et al., J. Nucl. Mater. 241–243 (1997) 1110.
[26] E. Abramov et al., J. Nucl. Mater. 175 (1990) 90.
[27] D.A. Thompson, R.G. Macaulay-Newcombe, CFFTP G-9585, Canadian Fusion Fuels Technology Project, 1996.
[28] P.M.S. Jones, R. Gibson, J. Nucl. Mater. 21 (1967) 353.
[29] G. Federici et al., J. Nucl. Mater. 227 (1996) 170.
[30] G. Federici et al., J. Nucl. Mater. 233–237 (1996) 741.
[31] G.R. Longhurst et al., EGG-FSP-10315, Idaho National Engineering and Environmental Laboratory, 1992.
[32] M.I. Baskes, DIFFUSE 83, SAND83-8231, Sandia National Laboratories, 1983.
[33] W. Möller, IPP 9/44, Max Planck Institut für Plasmaphysik, 1983.
[34] R.A. Causey, K.L. Wilson, J. Nucl. Mater. 212–215 (1994) 1436.
[35] H. Trinkaus, W.G. Wolfer, J. Nucl. Mater. 122/123 (1984) 552.
[36] H.H. Johnson, Scripta Metal. 23 (1989) 1703.
[37] G.A. Henshall et al., UCRL-ID120258, Lawrence Livermore National Laboratory, 1995.
[38] V.I. Shapovalov, Yu.M. Dukel'ski, Russian Metallurgy 5 (1984) 210.
[39] W.L. Hsu et al., J. Nucl. Mater. 176/177 (1990) 218.